Ⅳ. 研究成果の刊行物・別刷り

Biol Blood Marrow Transplant xxx (2014) 1–7

Biology of Blood and Marrow Transplantation

journal homepage: www.bbmt.org

ASBMT American Society for Blood and Marrow Transplantation

Choreito Formula for BK Virus–associated Hemorrhagic Cystitis after Allogeneic Hematopoietic Stem Cell Transplantation

Q5 Nozomu Kawashima, Yoshinori Ito, Yuko Sekiya, Atsushi Narita, Yusuke Okuno, Hideki Muramatsu, Masahiro Irie, Asahito Hama, Yoshiyuki Takahashi, Seiji Kojima*

Department of Pediatrics, Nagoya University Graduate School of Medicine, Nagoya, Japan

Article history:
Received 28 August 2014
Accepted 21 October 2014

Key Words:
BK virus
Hemorrhagic cystitis
Pediatric
Choreito
Kampo medicine

A B S T R A C T

Therapy for BK virus (BKV)–associated hemorrhagic cystitis (BKV-HC) is limited after hematopoietic stem cell transplantation (HSCT). We examined whether choreito, a formula from Japanese traditional Kampo medicine, is effective for treating BKV-HC. Among children who underwent allogeneic HSCT between October 2006 and March 2014, 14 were diagnosed with BKV-HC (median, 36 days; range, 14 to 330 days) after HSCT, and 6 consecutive children received pharmaceutical-grade choreito extract granules. The hematuria grade before treatment was significantly higher in the choreito group than in the nonchoreito group ($P = .018$). The duration from therapy to complete resolution was significantly shorter in the choreito group (median, 9 days; range, 4 to 17 days) than in the nonchoreito group (median, 17 days; range, 15 to 66 days; $P = .037$). In 11 children with macroscopic hematuria, the duration from treatment to resolution of macroscopic hematuria was significantly shorter in the choreito group than in the nonchoreito group (median, 2 days versus 11 days; $P = .0043$). The BKV load in urine was significantly decreased 1 month after choreito administration. No adverse effects related to choreito administration were observed. Choreito may be a safe and considerably promising therapy for the hemostasis of BKV-HC after HSCT.

INTRODUCTION

Hemorrhagic cystitis (HC) is a severe complication in patients undergoing hematopoietic stem cell transplantation (HSCT), resulting in significant morbidity, such as nephropathy and renal failure, prolonged hospitalization, and prolonged blood transfusion requirement [1,2]. Effects on mortality have also been reported in children undergoing HSCT [3]. Early-onset HC occurs within 1 week after HSCT and is mostly a symptom of regimen-related toxicity. Late-onset HC usually occurs after engraftment and is associated with viral infections, including those caused by the human polyomavirus BK (BKV), polyomavirus JC, adenovirus (AdV), and cytomegalovirus (CMV) [4]. BKV is the most frequent cause of late-onset HC and affects 5.3% to 21.2% of children undergoing HSCT [5-9]. BKV viruria is detected by real-time quantitative PCR (RT-PCR) in all patients with BKV-HC. A BKV load of more than 10^6 copies/mL in urine may be associated with a high risk of developing HC after HSCT [5]. However, asymptomatic BK viruria is detected in 50% to 100% of patients after HSCT [5,7,10], implicating that the presence of BKV viruria alone does not explain the pathogenesis of HC. High BKV viremia ($\geq 10^3$ copies/mL) is a better predictor of BKV-HC after HSCT, with a reported specificity of 93% [8]. Children with high BKV viremia ($\geq 10^4$ copies/mL) are at a higher risk of developing severe HC [6].

The standard treatment for BKV-HC has not been established [2]. Supportive therapy is provided to patients with mild BKV-HC, including intravenous hydration, bladder irrigation, and symptomatic relief treatment, such as the use of analgesics. Patients with severe BKV-HC require additional therapy. The current first line BKV-oriented therapy is intravenous cidofovir; however, its efficacy remains controversial [2]. Alternative strategies include intravesical instillation of cidofovir [2,7], hyperbaric oxygen therapy [11], leflunomide, and fluoroquinolone [12]; however, their effect is limited [13]. Invasive intervention such as vascular embolization or cystectomy may be necessary in uncontrollable HC.

Choreito is a formula derived from Japanese traditional Kampo medicine. The indication for choreito in the context of

Financial disclosure: See Acknowledgments on page 6.

* Correspondence and reprint requests: Seiji Kojima, MD, PhD, Department of Pediatrics, Nagoya University Graduate School of Medicine, 65 Tsurumai-cho, Showa-ku, Nagoya, Aichi, 466-8550 Japan.
E-mail address: kwnozomu@gmail.com (S. Kojima).

http://dx.doi.org/10.1016/j.bbmt.2014.10.018
1083-8791/

Kampo medicine is "dampness-heat" in the lower abdomen, the characteristic symptoms of which include dysuria, heat in the lower abdomen, and thirst. All these symptoms may be caused by inflammation and blood clots in the bladder. Based on this indication, choreito has been administered to patients with acute simple cystitis and urolithiasis, and its effectiveness has been confirmed [14]. Recently, choreito was successfully used to treat massive gross hematuria with clot retention in the bladder in a child with refractory acute lymphoblastic leukemia [14]. At present, choreito is covered by the national health insurance and is widely used for genitourinary symptoms in Japan.

Symptoms leading to the traditional use of choreito appear to overlap with symptoms associated with BKV-HC; indeed, some children receive choreito for HC. In this study, we retrospectively analyzed BKV-HC in children undergoing HSCT and evaluated the efficacy of choreito treatment.

PATIENTS AND METHODS

Definition

HC was defined as microscopic (blood in urine graded 1+ or more) or macroscopic hematuria combined with dysuria, pollakisuria, urinary urgency, and/or the sensation of residual urine in the absence of bacteria in urine as observed by culture [9]. *BKV-HC* was defined as the association of HC with BKV viruria and/or viremia. HC was graded according to the widely used criteria [15]. Grade I is defined as microscopic hematuria, grade II as macrohematuria, grade III as macroscopic hematuria with clots, and grade IV as macroscopic hematuria with renal or bladder dysfunction. The onset of BKV-HC was defined as the first day when patients presented with urinary symptoms, and *complete resolution* (CR) of HC was defined as blood in urine (− or + for hemoglobin) and disappearance of dysuria, pollakisuria, urinary urgency, and the sensation of residual urine related to HC.

Patient Inclusion Criteria of BKV-HC and Choreito Administration

Among the children (≤18 years old) who received allogeneic HSCT between October 2006 and March 2014 in Nagoya University Hospital, 14 were diagnosed with BKV-HC and included in the study. Their medical records were retrospectively analyzed. Patient characteristics are listed in Table 1. Intravenous fluids corresponding to 2.5 to 3.0 L/m^2/day with forced alkalinized diuresis were administered during conditioning, and patients treated with cyclophosphamide received prophylactic mesna for the prevention of HC. All the patients received acyclovir for herpes prophylaxis and weekly intravenous immunoglobulin for viral prophylaxis. Tacrolimus was intravenously administered for graft-versus-host disease (GVHD) prophylaxis in patients receiving HSCT from an unrelated donor. Cases of engraftment syndrome and GVHD were treated by methylprednisolone, followed by salvage therapies in nonresponding patients. Six children with BKV-HC diagnosed after March 2013 received a pharmaceutical-grade medicine, choreito extract granules (Tsumura & Co., Tokyo, Japan) with a dose of .2 g/kg per os daily in 3 divided doses (maximum, 7.5 g/day). Cidofovir and choreito were administered at the onset of macroscopic hematuria. Because it is not currently approved for clinical use in Japan, cidofovir was administered only to those who provided written informed consent.

Quantification of BKV DNA

Children undergoing HSCT were weekly monitored for plasma CMV, human herpesvirus 6, and Epstein-Barr virus, and those who met the criteria for HC underwent additional viral workup, including analysis for BKV, polyomavirus JC, and AdV. For 2 patients with BKV diagnosed before December 2009, BKV had been detected in urine by qualitative PCR. This qualitative PCR could not detect BKV in patients without HC. After January 2010, viruses were monitored by multiplex RT-PCR for quantification of DNA from BKV, polyomavirus JC, and AdV, as described previously [16]. In April 2010, BKV RT-PCR was used to screen all 30 hospitalized children with various hemato-oncological diseases who had neither HC-related symptoms nor abnormal urinalysis. All patients provided informed consent for viral PCR workup in accordance with the Declaration of Helsinki. This retrospective analysis was approved by the ethics committee of Nagoya University Graduate School of Medicine.

Statistical Analysis

Statistical analysis was performed using the Fisher's exact test for categorical variables and the Mann-Whitney's *U* test for continuous variables. The Wilcoxon signed-rank test was used for paired samples. Odds ratios with confidence intervals were estimated by the logistic regression. A probability (*P*) value <.05 was considered to indicate statistical significance. All statistical analyses were conducted using JMP Pro 11.0.0 (SAS Institute Inc., Cary, NC).

RESULTS

BKV Screening in Hemato-oncological Patients without Genitourinary Symptoms

All children with hemato-oncological disorders hospitalized in the same ward were screened for BKV viruria for the purpose of surveillance. BKV viruria was detected in 5 (17%) of 30 hospitalized children with various hemato-oncological diseases who had neither HC-related symptoms nor abnormal urinalysis. The median urine BKV load in children with asymptomatic viruria was 1.3×10^6 copies/mL (range, 3.5×10^3 to 2.0×10^9 copies/mL), which was significantly lower than that in children with BKV-HC (median, 5.4×10^{10} copies/mL; range, 8.3×10^7 to 1.5×10^{11} copies/mL; $P = .0021$).

Patient Characteristics of Cases with BKV-HC after HSCT

Table 1 summarizes the patient characteristics of 14 children who underwent HSCT and later developed BKV-HC. In patients 1 and 2, BKV was detected in urine by qualitative

Table 1
Patient Demographics of BKV-HC after HSCT

UPN	Choreito Treatment	Age, yr	Sex	Diagnosis	Clinical Status	Preconditioning Regimen	Stem Cell Source	GVHD Prophylaxis
1	No	15.3	M	AA	Non CR	CY + ATG + TBI 5 Gy	UR-BM	FK + sMTX
2	No	16.0	M	AA	Non CR	FLU + CY + Campath + TBI 3 Gy	UR-BM	FK + sMTX
3	No	12.3	M	B-ALL	CR1	MEL + TBI 12 Gy	UR-BM	FK + sMTX
4	No	11.8	M	CML	CyCR	FLU + MEL + TBI 3 Gy	UR-BM	FK + sMTX
5	No	7.1	F	T-ALL	CR2	FLU + MEL + ATG + TBI 12 Gy	Haplo	FK + sMTX
6	No	5.7	M	NB	CR1	FLU + MEL + TBI 2 Gy	UR-CB	FK + sMTX
7	No	15.4	M	CMML	Non CR	FLU + MEL + ATG + TBI 5 Gy	Haplo	FK + sMTX
8	No	7.8	M	B-ALL	CR2	MEL + ATG + TBI 12 Gy	UR-BM	FK + sMTX
9	Yes	14.3	M	AA	Non CR	FLU + MEL + ATG + TBI 3 Gy	Haplo	FK + sMTX
10	Yes	5.4	M	MDS	Non CR	FLU + MEL + ATG + TBI 5 Gy	Haplo	FK + sMTX
11	Yes	10.1	F	AA	Non CR	FLU + MEL + ATG + TBI 5 Gy	Haplo	FK + sMTX
12	Yes	12.2	F	CMML	Non CR	FLU + MEL + ATG + TBI 5 Gy	Haplo	FK + sMTX
13	Yes	6.8	M	B-ALL	CR2	MEL + TBI 12 Gy	UR-BM	FK + sMTX
14	Yes	7.5	M	MDS	Non CR	FLU + MEL + ATG + TBI 5 Gy	Haplo	FK + sMTX

UPN indicates unique patient number; M, male; AA, aplastic anemia; Cy, cyclophosphamide; ATG, antithymocyte globulin; TBI, total body irradiation; UR, unrelated; BM, bone marrow; FK, tacrolimus; sMTX, short course of methotrexate; FLU, fludarabine; Campath, alemtuzumab; ALL, acute lymphoblastic leukemia; MEL, melphalan; CML, chronic myelogenous leukemia; CyCR, cytological complete remission; F, female; Haplo, haploidentical transplant; NB, neuroblastoma; CB, cord blood; CMML, chronic myelomonocytic leukemia; MDS, myelodysplastic syndrome.

PCR; therefore, other agents including preconditioning could have contributed to HC. Six of the 14 children received choreito because of BKV-HC. All patients were older than 5 years (median, 11 years; range, 5.4 to 16 years). Antithymoglobulin or alemtuzumab was administered to 10 of 14 children (71%) as a preconditioning. Notably, all the children received total body irradiation with various doses.

Children were diagnosed with BKV-HC at a median 36 days (range, 14 to 330 days) (Table 2) after HSCT. Six of 14 patients (43%) had grade II to IV acute GVHD, and 11 of 14 (79%) received steroids for treatment of engraftment syndrome and/or acute GVHD before being diagnosed with BKV-HC. Three children with acute GVHD grade III or IV received intensified immunosuppressive treatment for steroid-resistant GVHD; 1 received infliximab and the other 2 received infliximab, basiliximab, and mesenchymal stem cells. All 3 responded well to additional therapy for acute GVHD. Concomitant AdV viruria was detected in 2 of 14 children (14%), and 12 of 14 children (86%) developed CMV and/or Epstein-Barr virus infection after HSCT. AdV titers in the urine were 2.6×10^8 copies/mL in patient 3 and 1.8×10^8 copies/mL in patient 7 at the time of diagnosis. CMV viruria was not detected in any of these 14 children when BKV-HC was diagnosed. Six children were receiving gancyclovir and/or foscarnet for CMV reactivation at the time of BKV-HC diagnosis.

Treatment for BKV Cystitis with Choreito

Six of 14 children with BKV-HC diagnosed after October 2013 received choreito (Tables 1 to 3). All 6 fulfilled the Kampo indication for receiving choreito ("lower energizer dampness-heat" in patients 9, 11, 12, 13, and 14, and "heat binding in the lower energizer" in patient 10). Patient characteristics, including age at HSCT, sex, underlying disease, engraftment syndrome, acute GVHD frequency and grade, immunosuppressive treatment, absolute lymphocyte count, antiviral therapy, duration of steroid use before the diagnosis of BKV-HC, and duration from HSCT to the onset of BKV-HC, did not differ significantly between the choreito group and the nonchoreito group (Tables 1 and 2). However, the hematuria grade at the time of diagnosis of BKV-HC was significantly higher in the choreito group than in the nonchoreito group ($P = .018$) (Table 2). Choreito was administered over a median of 5 days after the onset of symptoms related to BKV-HC (range, 2 to 16 days), and this interval was not statistically different from that of other treatments (median, 4 days; range, 1 to 23 days; $P = .43$) (Table 3). The urine BKV load before treatment amounted to a median of 2.6×10^{10} copies/mL (range, 1.3×10^9 to 6.3×10^{10} copies/mL) in children receiving choreito, which was not statistically different from that in those not receiving choreito (median, 3.4×10^{10} copies/mL; range, 8.3×10^7 to 1.3×10^{11} copies/mL; $P = .67$) (Table 3). Similarly, the BKV load in whole blood before treatment was not statistically different between the choreito and nonchoreito groups ($P = .24$, Table 3).

In all 14 children with BKV-HC, the duration from the start of therapy to CR as defined by disappearance of dysuria, pollakisuria, urinary urgency, and the sensation of residual urine was significantly shorter in the choreito group (median, 9 days; range, 4 to 17 days) than in the nonchoreito group (median, 17 days; range, 15 to 66 days; $P = .037$) (Table 3, Figure 1A): the odds ratio of choreito versus nonchoreito was .63 (95% confidence interval, .22 to .93; $P = .0031$). With regard to 11 children with HC graded ≥ II at the beginning of therapy, the administration of choreito

Table 2
Clinical Characteristics of Patients with BKV Cystitis

UPN	Engraftment Syndrome	Acute GVHD		ALC at the Diagnosis of BKV-HC ($\times 10^9$/L)	Steroid Use (d before BKV-HC)	Other Immunosuppressants	Onset of BKV-HC (d from SCT)	Hematuria (Grade)	Viruria (Urine log copy/mL)	CMV (Whole Blood log copy/mL)	Viral Infections	Antiviral Therapy at BKV-HC
		Stage	Grade									
1	+	-	-	4.7	14	-	35	II	BKV	0.0	CMV, EBV	GCV
2	-	skin 3	II	.3	24	-	65	II	BKV	3.1	CMV	PFA
3	+	-	-	.8	10	-	36	III	BKV (9.2), AdV (8.4)	0.0	CMV	PFA
4	+	skin 3	II	1	90	-	330	II	BKV (7.9)	0.0	CMV, EBV	PFA
5	+	skin 2, gut 1	II	.2	-	-	14	II	BKV (10.8)	2.6	CMV	-
6	-	skin 2, gut 3	III	1	10	INX	45	I	BKV (10.9)	0.0	-	-
7	-	skin 3, gut 2	III	.6	67	INX, BSX, MSC	86	I	BKV (11.1), AdV (8.3)	3.0	CMV, EBV	-
8	+	-	-	2	2	-	27	II	BKV (10.0)	3.2	CMV	-
9	-	-	-	.2	-	-	16	III	BKV (9.1)	2.9	EBV	-
10	+	skin 2, liver 4, gut 2	IV	.8	12	INX, BSX, MSC	25	III	BKV (9.2)	0.0	-	-
11	+	-	-	1.8	30	-	48	III	BKV (9.5)	0.0	CMV, EBV	GCV + PFA
12	+	-	-	.2	45	-	67	III	BKV (10.8)	2.7	CMV	GCV
13	-	-	-	1.3	-	-	21	III	BKV (10.7)	0.0	CMV	-
14	+	-	-	.5	6	-	26	I	BKV (10.7)	0.0	EBV	-

ALC indicates absolute lymphocyte count; SCT, stem cell transplanation; EBV, Epstein-Barr virus; GCV, gancyclovir; PFA, foscarnet; INX, infliximab; BSX, basiliximab; MSC, mesenchymal stem cell transplantation.

Table 3
Summary of Treatment for Patients with BKV Cystitis

UPN	Duration from Onset to Tx, d	Primary Tx for BKV	Hematuria Grade at Tx	Hematuria Grade ≤I (d from Tx)	CR (d from Tx)	Urine BKV Load before Tx (log copy/mL)	Plasma BKV Load before Tx (log copy/mL)	Urine BKV Load 1 mo after Tx (log copy/mL)	Plasma BKV Load 1 mo after Tx (log copy/mL)	Possible Complications
1	7	Cidofovir (5 mg/kg qwk ×2), hydration	II	11	17	N/A	N/A	N/A	N/A	None
2	4	Bladder irrigation, hydration	II	16	55	N/A	N/A	N/A	N/A	None
3	14	Cidofovir (1 mg/kg qwk ×2), hydration	III	28	66	9.2	0.0	6.5	3.8	Renal failure
4	4	Hydration	II	10	15	7.9	0.0	N/A	N/A	None
5	2	Hydration	II	5	16	10.8	0.0	N/A	N/A	None
6	1	Hydration	I	N/A	15	10.9	3.0	10.5	3.6	None
7	1	Hydration	I	N/A	15	11.1	0.0	N/A	N/A	None
8	23	Hydration	II	8	23	10.0	0.0	N/A	N/A	None
9	16	Choreito, cidofovir (1 mg/kg qwk ×11), hydration	III	4	6	9.1	4.0	8.7	4.6	None
10	5	Choreito	III	2	4	9.2	3.1	8.3	4.0	None
11	2	Choreito	III	2	16	9.5	0.0	7.8	0.0	None
12	4	Choreito	III	3	17	10.8	0.0	8.2	5.8	None
13	5	Choreito	III	2	7	10.7	5.0	4.4	0.0	None
14	16	Choreito	I	N/A	11	10.7	2.1	10.5	3.2	None

Tx indicates treatment; qwk, every week; N/A, not applicable or available.

significantly shortened the duration from the onset to BKV-HC grade ≤ I (median, 2 days; range, 2 to 4 days) in comparison with that in the nonchoreito group (median, 11 days; range, 5 to 28 days; $P = .0043$) (Table 3, Figure 1B). The duration from start of therapy to CR was also significantly shorter in the choreito group (median, 7 days; range, 4 to 17 days) than in the nonchoreito group (median, 20 days; range, 15 to 66 days; $P = .048$) (Table 3, Figure 1C): here, the odds ratio of choreito versus nonchoreito was .66 (95% confidence interval, .14 to .95; $P = .0058$).

Sequential Analysis of BKV Load after Choreito Treatment

BKV-HC–related symptoms improved significantly earlier in children receiving choreito, and we studied whether these earlier improvements were related to the clearance of BKV. The BKV load in urine and whole blood was monitored after the diagnosis of BKV-HC in children receiving choreito. The urine BKV load generally decreased over time. The median urine BKV load was 1.7×10^8 copies/mL (range, 2.6×10^4 to 3.1×10^{10} copies/mL) 1 month after BKV-HC diagnosis when all children had achieved CR, and they experienced a statistically significant decrease in BKV load since the time of diagnosis ($P = .031$; Wilcoxon signed-rank test for paired samples) (Table 3, Figure 2A). At the time of CR, only 1 of 6 children had a urine BKV load lower than 1.3×10^6 copies/mL, which was the median urine BKV load in children with asymptomatic viruria. The BKV load in whole blood appeared stable during the course of BKV-HC, and no significant decrease was observed a month after diagnosis ($P = .44$) (Table 3, Figure 2B).

All 6 children eventually finished taking choreito, and relapse of HC was not observed, except for in 1 patient who experienced relapse twice (patient 9). This patient was diagnosed with idiopathic aplastic anemia and received a bone marrow transplant from an unrelated donor; however, the graft was rejected and he underwent haplo-identical HSCT as the second HSCT. Because he developed chronic GVHD, he was administered prednisolone, which was increased during the exacerbation of chronic GVHD and which may have contributed to the prolonged elevation of the BKV load. Every time the patient had a relapse of BKV-HC, he was administered choreito, and his genitourinary symptoms resolved within a few days (Supplemental Figure 1).

Safety and Tolerability of Treatment

All children were able to take choreito per os. Notably, there were no adverse effects due to choreito intake, and renal function impairment was not observed in children receiving choreito (Table 3). The reported adverse effects of choreito include drug allergy and mild gastric discomfort [14], which were not observed in any of the children. In the nonchoreito group, 1 patient (patient 3) who received cidofovir for BKV infection developed impaired renal function, possibly resulting from renal toxicity of cidofovir and postrenal acute kidney injury due to clot retention.

DISCUSSION

Unlike its effect in immunocompetent patients, HC is life threatening in immunocompromised patients with hemato-oncological disease, particularly among patients undergoing HSCT [17]. To our knowledge, prospective studies of the treatment for BKV-HC are not available, and there are no standard treatment guidelines for post-HSCT HC. Treatment modalities are limited, particularly in children, partly owing to few reports on children receiving pharmaceutical and

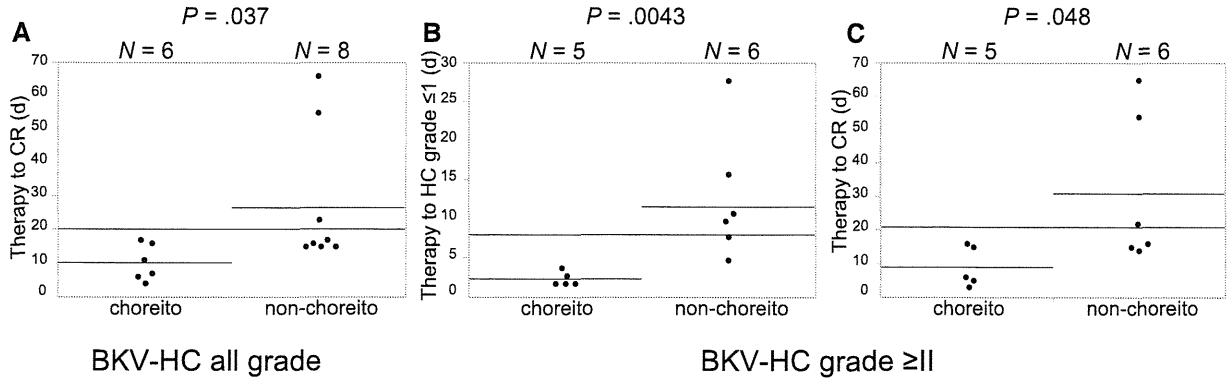

Figure 1. Comparison of choreito and nonchoreito treatment for BK virus-associated hemorrhagic cystitis (BKV-HC). The duration from the beginning of therapy to complete resolution (CR), as defined by the absence of dysuria, pollakisuria, urinary urgency, or the sensation of residual urine, was shorter in the choreito group (median, 9 days; range, 4 to 17 days) than in the nonchoreito group (median, 17 days; range, 15 to 66 days; $P = .037$) (A). When comparing children with HC graded ≥ II, the administration of choreito significantly shortened the duration from the onset to BKV-HC grade ≤ I (median, 2 days; range, 2 to 4 days) in comparison with that in the nonchoreito group (median, 11 days; range, 5 to 28 days) (B). The duration from start of therapy to CR was also significantly shorter in the choreito group (median, 7 days; range, 4 to 17 days) than in the nonchoreito group (median, 20 days; range, 15 to 66 days; $P = .048$) (C).

surgical treatments [4,18-20]. Intravenous hydration with forced diuresis is conducted; however, this is supportive treatment only without reliable efficacy.

At present, cidofovir is the only commercially available antiviral agent against BKV, and its efficacy for BKV-HC has been investigated only in retrospective studies [19-21]. In the report from the European Group for Blood and Marrow Transplantation, intravenous or intravesical cidofovir was administered to 62 patients with BKV-HC [21]. Of the 62 patients, 41 (66%) achieved CR and 8 (13%) had partial response after cidofovir treatment; however, no improvement or deterioration was observed in 12 patients (19%). CR is related to clearance of BK viremia in patients with BK viremia detected at the beginning of treatment, and the median time to clearance is 37 days (range, 7 to 102 days). Of 57 patients receiving intravenous cidofovir, 17 (30%) experienced renal toxicity. In a pediatric cohort, 19 children received cidofovir for BKV-HC grade ≥ II [19]. Macroscopic hematuria resolved in 15 (79%) after a median of 22 days (range, 9 to 63 days). In 1 patient, HC progressed to grade IV during cidofovir treatment. Notably, the baseline creatinine level appeared to be elevated after treatment. Another pediatric cohort included 12 children with BKV-HC treated by intravenous and/or intravesical cidofovir [20]. The median duration of symptoms was 25 days (range, 9 to 73 days) and no persistent nephrotoxicity was observed. Compared with cidofovir treatment, children treated with choreito treatment in our study experienced no impairment of renal function; all patients with BKV-HC achieved CR and BKV-HC resolved earlier.

Hyperbaric oxygen therapy is another alternative treatment for BKV-HC [11,22]. A retrospective study included 16 patients with BKV-HC grade ≥ II (5 patients under 19 years of age), 15 (94%) of whom achieved CR after a median of 17 days (range, 4 to 116 days) [11]. In a pediatric cohort of 10 children with BKV-HC grade ≥ II, 9 (90%) achieved CR after a median of 15 days (range, 10 to 37 days), including spontaneous resolution [22]. Hyperbaric oxygen is generally well tolerated; however, it requires a high-cost facility and adverse effects have been reported, including ruptured tympanum.

Other alternative therapies include leflunomide and fluoroquinolone antibiotics [12]; however, experience is limited, even in adults [13]. Few reports of leflunomide use in the setting of HSCT are available and its safety has not been

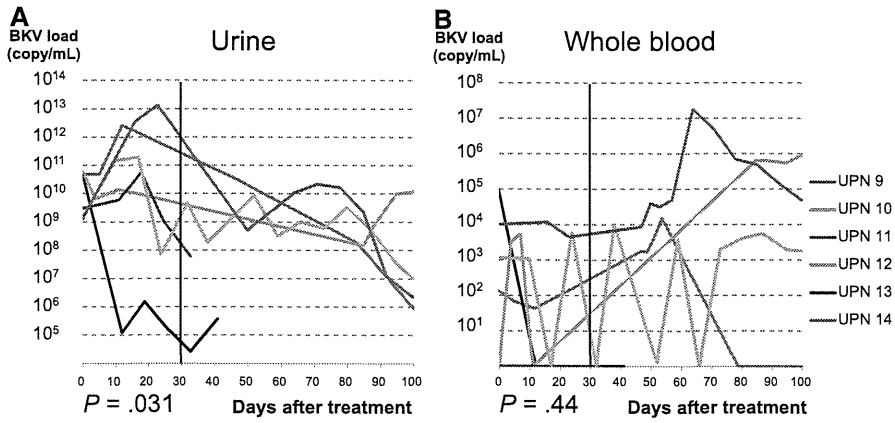

Figure 2. BK virus (BKV) load after choreito treatment. The BKV load before treatment amounted to a median of 2.6×10^{10} copies/mL in urine (range, 1.3×10^{9} to 6.3×10^{10} copies/mL) and a median of 6.5×10^{2} copies/mL in whole blood (range, 0 to 9.0×10^{4} copies/mL). The median urine BKV load was 1.7×10^{8} copies/mL (range, 2.6×10^{4} to 3.1×10^{10} copies/mL) 1 month after BKV-HC diagnosis, and the BKV load had significantly decreased since the time of diagnosis (Wilcoxon signed-rank test, $P = .031$) (A). The BKV load in whole blood appeared stable during the course of BKV-HC, and no significant decrease was observed a month after diagnosis (Wilcoxon signed-rank test, $P = .44$) (B).

confirmed in children. Fluoroquinolones are historically contraindicated in children because they cause arthrotoxicity in juvenile animals and are associated with reversible musculoskeletal events in both children and adults; therefore, they are not recommended in the absence of convincing evidence.

Choreito is a formula stemming from Japanese traditional (Kampo) medicine, originally developed from traditional Chinese medicine; it was the orthodox medicine in Japan until the 19th century, when modern Western medicine took over [14]. Nevertheless, some Kampo formulae are still officially registered in the Japanese Pharmacopoeia. Although Kampo extracts are crude drugs derived from plants, animals, and minerals, their quality is strictly controlled in accordance with the Japanese Pharmacopoeia by quantitative analysis of marker components using high-performance liquid chromatography. Kampo formulae are classified as dietary supplements outside Japan and are approved for marketing by the Food and Drug Administration in the United States.

Choreito is a crude product from *Polyporus umbellatus* sclerotium, *Wolfiporia extensa* sclerotium, *Alisma orientale* rhizome, aluminum silicate hydrate with silicon dioxide, and glue. Ergone isolated from *P. umbellatus* prevented early renal injury in a rat model of nephropathy [23] and may play a central role in the effect exerted by choreito. Pollakisuria was ameliorated in 93% of patients who received choreito for lower urinary tract symptoms in an open-label, single-arm study of 30 patients [24]. Choreito was also administered to patients with urolithiasis for enhancing the evacuation of stones after extracorporeal shock wave lithotripsy [25]. In these studies, no severe adverse effects were observed, suggesting high safety of choreito.

Considering the wide range of indications in genitourinary disorders, choreito may protect epithelial cells irrespective of the type of pathogens and thereby be an effective treatment option for the hemostasis of HC. Although the precise pathogenesis of BKV-HC remains unclear, urothelial cells infected with BKV in vitro detached without causing local cell lysis, which may be associated with the denudation of the damaged mucosa in patients with BKV-HC [26]. Choreito may protect urothelial cells from detaching, which may result in a significant reduction of the BKV load in urine, although the whole blood BKV load appears unchanged and the BKV burden itself is not reduced. Notably, unlike other antiviral agents or surgical interventions, no adverse effects were observed during choreito administration, although the mechanism of action of choreito remains unclear; hence, its safety cannot be easily predicted.

Our study has some limitations. The small number of study subjects in this single-center retrospective analysis may result in bias. Five of 8 subjects in the nonchoreito group had grade II to III GVHD, whereas 1 out of 6 subjects in the choreito group had grade IV GVHD. This difference in GVHD frequency could have been a contributing factor for the difference in HC severity and BKV clearance, although it was not statistically different ($P = .14$) among the 2 groups, possibly because of the small sample size. Children with concomitant AdV viruria were included only in the nonchoreito group, which may explain the longer time before CR in the non-
Q2 choreito group. In the present study, HC was significantly more severe in the choreito group than the nonchoreito group. This difference may represent the difference in preconditioning and donor sources: the choreito group included more cases of haplo-identical HSCT, which may have resulted in intensified immunosuppression. More severe HC correlates with a longer duration of HC [2]. Nevertheless, the duration of HC was significantly shorter in the choreito group, which exemplifies its effectiveness. Although the urine BKV load had significantly decreased 1 month after choreito treatment examined by the paired samples, this decrease could not be compared with that of the nonchoreito group because of a lack of paired samples in most of the patients in the nonchoreito group. Thus, the impact of choreito treatment on the urine BV virus load should be investigated in a prospective study where the BKV load is sequentially followed for every study subject.

In conclusion, choreito may be a safe and effective therapy for the hemostasis of late-onset BKV-HC following HSCT, although it may not decrease the BKV burden. Although its precise mechanism of hemostasis remains unclear, choreito may be administered as the first-line treatment for post-HSCT HC. Prospective, randomized studies are warranted to confirm the efficacy of choreito in the treatment of BKV-HC. Fundamental research aiming to identify the active ingredients and mechanisms of action is also essential.

ACKNOWLEDGMENTS

The authors thank Fumiyo Ando, Yoshie Miura, Yinyan Xu, and Xinan Wang for their professional assistance.

Financial disclosure: Dr. Seiji Kojima received a research grant from Sanofi K.K. The other authors have no conflicts of Q3 interest to disclose.

SUPPLEMENTARY DATA

Supplementary data related to this article can be found online at http://dx.doi.org/10.1016/j.bbmt.2014.10.018.

REFERENCES

1. Lee YJ, Zheng J, Kolitsopoulos Y, et al. Relationship of BK polyoma virus (BKV) in the urine with hemorrhagic cystitis and renal function in recipients of T cell-depleted peripheral blood and cord blood stem cell transplantations. *Biol Blood Marrow Transplant.* 2014;20:1204-1210.
2. Gilis L, Morisset S, Billaud G, et al. High burden of BK virus-associated hemorrhagic cystitis in patients undergoing allogeneic hematopoietic stem cell transplantation. *Bone Marrow Transplant.* 2014;49:664-670.
3. Haines HL, Laskin BL, Goebel J, et al. Blood, and not urine, BK viral load predicts renal outcome in children with hemorrhagic cystitis following hematopoietic stem cell transplantation. *Biol Blood Marrow Transplant.* 2011;17:1512-1519.
4. Decker DB, Karam JA, Wilcox DT. Pediatric hemorrhagic cystitis. *J Pediatr Urol.* 2009;5:254-264.
5. Megged O, Stein J, Ben-Meir D, et al. BK-virus-associated hemorrhagic cystitis in children after hematopoietic stem cell transplantation. *J Pediatr Hematol Oncol.* 2011;33:190-193.
6. Oshrine B, Bunin N, Li Y, et al. Kidney and bladder outcomes in children with hemorrhagic cystitis and BK virus infection after allogeneic hematopoietic stem cell transplantation. *Biol Blood Marrow Transplant.* 2013;19:1702-1707.
7. Laskin BL, Denburg M, Furth S, et al. BK viremia precedes hemorrhagic cystitis in children undergoing allogeneic hematopoietic stem cell transplantation. *Biol Blood Marrow Transplant.* 2013;19:1175-1182.
8. Cesaro S, Facchin C, Tridello G, et al. A prospective study of BK-virus-associated haemorrhagic cystitis in paediatric patients undergoing allogeneic haematopoietic stem cell transplantation. *Bone Marrow Transplant.* 2008;41:363-370.
9. Kloos RQ, Boelens JJ, de Jong TP, et al. Hemorrhagic cystitis in a cohort of pediatric transplantations: incidence, treatment, outcome, and risk factors. *Biol Blood Marrow Transplant.* 2013;19:1263-1266.
10. Drew RJ, Walsh A, Ní Laoi B, et al. BK virus (BKV) plasma dynamics in patients with BKV-associated hemorrhagic cystitis following allogeneic stem cell transplantation. *Transpl Infect Dis.* 2013;15:276-282.
11. Savva-Bordalo J, Pinho Vaz C, Sousa M, et al. Clinical effectiveness of hyperbaric oxygen therapy for BK-virus-associated hemorrhagic cystitis after allogeneic bone marrow transplantation. *Bone Marrow Transplant.* 2012;47:1095-1098.
12. Zaman RA, Ettenger RB, Cheam H, et al. A novel treatment regimen for BK viremia. *Transplantation.* 2014;97:1166-1171.

13. Harkensee C, Vasdev N, Gennery AR, et al. Prevention and management of BK-virus associated haemorrhagic cystitis in children following haematopoietic stem cell transplantation—a systematic review and evidence-based guidance for clinical management. *Br J Haematol.* 2008;142:717-731.
14. Kawashima N, Deveaux TE, Yoshida N, et al. Choreito, a formula from Japanese traditional medicine (Kampo medicine), for massive hemorrhagic cystitis and clot retention in a pediatric patient with refractory acute lymphoblastic leukemia. *Phytomedicine.* 2012;19:1143-1146.
15. Droller MJ, Gomolka D. Expression of the cellular immune response during tumor development in an animal model of bladder cancer. *J Urol.* 1982;128:1385-1389.
16. Funahashi Y, Iwata S, Ito Y, et al. Multiplex real-time PCR assay for simultaneous quantification of BK polyomavirus, JC polyomavirus, and adenovirus DNA. *J Clin Microbiol.* 2010;48:825-830.
17. Hale GA, Rochester RJ, Heslop HE, et al. Hemorrhagic cystitis after allogeneic bone marrow transplantation in children: clinical characteristics and outcome. *Biol Blood Marrow Transplant.* 2003;9:698-705.
18. Hassan Z. Management of refractory hemorrhagic cystitis following hematopoietic stem cell transplantation in children. *Pediatr Transplant.* 2011;15:348-361.
19. Gorczynska E, Turkiewicz D, Rybka K, et al. Incidence, clinical outcome, and management of virus-induced hemorrhagic cystitis in children and adolescents after allogeneic hematopoietic cell transplantation. *Biol Blood Marrow Transplant.* 2005;11:797-804.
20. Kwon HJ, Kang JH, Lee JW, et al. Treatment of BK virus-associated hemorrhagic cystitis in pediatric hematopoietic stem cell transplant recipients with cidofovir: a single-center experience. *Transpl Infect Dis.* 2013;15:569-574.
21. Cesaro S, Hirsch HH, Faraci M, et al. Cidofovir for BK virus-associated hemorrhagic cystitis: a retrospective study. *Clin Infect Dis.* 2009;49:233-240.
22. Zama D, Masetti R, Vendemini F, et al. Clinical effectiveness of early treatment with hyperbaric oxygen therapy for severe late-onset hemorrhagic cystitis after hematopoietic stem cell transplantation in pediatric patients. *Pediatr Transplant.* 2013;17:86-91. Q4
23. Zhao YY, Zhang L, Mao JR, et al. Ergosta-4,6,8(14),22-tetraen-3-one isolated from Polyporus umbellatus prevents early renal injury in aristolochic acid-induced nephropathy rats. *J Pharm Pharmacol.* 2011;63:1581-1586.
24. Horii A, Maekawa M. Clinical evaluation of chorei-to and chorei-to-go-shimotsu-to in patients with lower urinary tract symptoms [article in Japanese]. *Hinyokika Kiyo.* 1988;34:2237-2241.
25. Wada S, Yoshimura R, Yamamoto K, et al. Effect of herbal drug, choreito, after extracorporeal shock wave lithotripsy on spontaneous stone delivery. *Jpn J Endourol ESWL.* 2001;14:155-158.
26. Li R, Sharma BN, Linder S, et al. Characteristics of polyomavirus BK (BKPyV) infection in primary human urothelial cells. *Virology.* 2013;440:41-50.

bjh research paper

Loss of function mutations in *RPL27* and *RPS27* identified by whole-exome sequencing in Diamond-Blackfan anaemia

RuNan Wang,[1] Kenichi Yoshida,[2,3] Tsutomu Toki,[1] Takafumi Sawada,[4] Tamayo Uechi,[4] Yusuke Okuno,[2,3] Aiko Sato-Otsubo,[2,3] Kazuko Kudo,[5] Isamu Kamimaki,[6] Rika Kanezaki,[1] Yuichi Shiraishi,[7] Kenichi Chiba,[7] Hiroko Tanaka,[8] Kiminori Terui,[1] Tomohiko Sato,[1] Yuji Iribe,[9] Shouichi Ohga,[10] Madoka Kuramitsu,[11] Isao Hamaguchi,[11] Akira Ohara,[12] Junichi Hara,[13] Kumiko Goi,[14] Kousaku Matsubara,[15] Kenichi Koike,[16] Akira Ishiguro,[17] Yasuhiro Okamoto,[18] Kenichiro Watanabe,[19] Hitoshi Kanno,[9] Seiji Kojima,[20] Satoru Miyano,[7,8] Naoya Kenmochi,[4] Seishi Ogawa[2,3] and Etsuro Ito[1]

[1]Department of Paediatrics, Hirosaki University Graduate School of Medicine, Hirosaki, [2]Cancer Genomics Project, Graduate School of Medicine, The University of Tokyo, Tokyo, [3]Department of Pathology and Tumour Biology, Graduate School of Medicine, Kyoto University, Kyoto, [4]Frontier Science Research Centre, University of Miyazaki, Miyazaki, [5]Division of Haematology and Oncology, Shizuoka Children's Hospital, Shizuoka, [6]Department of Paediatrics, Saitama National Hospital, Wako, [7]Laboratory of DNA Information Analysis, Human Genome Centre, Institute of Medical Science, The University of Tokyo, [8]Laboratory of Sequence Analysis, Human Genome Centre, Institute of Medical Science, The University of Tokyo, [9]Department of Transfusion Medicine and Cell Processing, Tokyo Women's Medical University, Tokyo, [10]Department of Perinatal and Paediatric Medicine, Graduate School of Medical Sciences, Kyushu University, Fukuoka, [11]Department of Safety Research on Blood and Biological Products, National Institute of Infectious Diseases, [12]Department of Transfusion, Omori Hospital, Toho University, Tokyo, [13]Department of Haematology and Oncology, Osaka City General Hospital, Osaka, [14]Department of Paediatrics, University of Yamanashi, Kofu, [15]Department of Paediatrics, Nishi-Kobe Medical Centre,Kobe, [16]Department of Paediat-

Summary

Diamond-Blackfan anaemia is a congenital bone marrow failure syndrome that is characterized by red blood cell aplasia. The disease has been associated with mutations or large deletions in 11 ribosomal protein genes including *RPS7*, *RPS10*, *RPS17*, *RPS19*, *RPS24*, *RPS26*, *RPS29*, *RPL5*, *RPL11*, *RPL26* and *RPL35A* as well as *GATA1* in more than 50% of patients. However, the molecular aetiology of many Diamond-Blackfan anaemia cases remains to be uncovered. To identify new mutations responsible for Diamond-Blackfan anaemia, we performed whole-exome sequencing analysis of 48 patients with no documented mutations/deletions involving known Diamond-Blackfan anaemia genes except for *RPS7*, *RPL26*, *RPS29* and *GATA1*. Here, we identified a *de novo* splicing error mutation in *RPL27* and frameshift deletion in *RPS27* in sporadic patients with Diamond-Blackfan anaemia. *In vitro* knockdown of gene expression disturbed pre-ribosomal RNA processing. Zebrafish models of *rpl27 and rps27* mutations showed impairments of erythrocyte production and tail and/or brain development. Additional novel mutations were found in eight patients, including *RPL3L*, *RPL6*, *RPL7L1T*, *RPL8*, *RPL13*, *RPL14*, *RPL18A* and *RPL31*. In conclusion, we identified novel germline mutations of two ribosomal protein genes responsible for Diamond-Blackfan anaemia, further confirming the concept that mutations in ribosomal protein genes lead to Diamond-Blackfan anaemia.

Keywords: bone marrow failure, Diamond-Blackfan, genetic analysis, erythropoiesis, childhood.

 doi: 10.1111/bjh.13229

rics, Shinshu University School of Medicine, Matsumoto, [17]Division of Haematology, National Centre for Child Health and Development, Tokyo, [18]Department of Paediatrics, Kagoshima University, Kagoshima, [19]Department of Paediatrics, Graduate School of Medicine, Kyoto University, Kyoto, and [20]Department of Paediatrics, Nagoya University Graduate School of Medicine, Nagoya, Japan

Received 21 August 2014; accepted for publication 7 October 2014
Correspondence: Professor Etsuro Ito, Department of Paediatrics, Hirosaki University Graduate School of Medicine, 53 Honcho, Hirosaki 036-8562, Japan.
E-mail: eturou@cc.hirosaki-u.ac.jp

Professor Seishi Ogawa, Cancer Genomics Project, Graduate School of Medicine, The University of Tokyo, 7-3-1, Hongo, Bunkyo-ku, Tokyo 113-8654, Japan.
E-mail: sogawa-tky@umin.ac.jp

Diamond-Blackfan anaemia (DBA) is an inherited rare red blood cell aplasia that is characterized by normochromic macrocytic anaemia, reticulocytopenia and selective defects in erythroid progenitor cells in normocellular bone marrow. Patients usually present with anaemia in the first year of life, although there is a non-classical mild phenotype diagnosed later in life. Macrocytic anaemia is a prominent feature of DBA but the disease is also characterized by growth retardation and congenital anomalies, including craniofacial, upper limb/hand, cardiac and genitourinary malformations, that are present in approximately half of the patients. In addition, DBA patients have a predisposition to malignancies including acute myeloid leukaemia, myelodysplastic syndrome, colon carcinoma, osteogenic sarcoma and female genital cancer (Lipton *et al*, 2006; Vlachos *et al*, 2008, 2012; Ito *et al*, 2010).

DBA is associated with single, monoallelic, inactivating mutations in ribosomal protein (RP) genes. Except for rare germline *GATA1* mutations reported in two X-linked DBA families (Sankaran *et al*, 2012), all known causative mutations have involved RP genes. Approximately 20% of DBA patients are familial. However, most cases occur sporadically and have *de novo* mutations. In DBA, mutations in RP genes include *RPS7*, *RPS10*, *RPS17*, *RPS19*, *RPS24*, *RPS26* and *RPS29* (encoding RP for the small subunit) and *RPL5*, *RPL11*, *RPL26* and *RPL35A* (encoding RP for the large subunit). These mutations have been reported in up to 60% of DBA patients (Draptchinskaia *et al*, 1999; Gazda *et al*, 2006, 2008, 2012; Cmejla *et al*, 2007; Farrar *et al*, 2008; Doherty *et al*, 2010; Konno *et al*, 2010; Gerrard *et al*, 2013; Mirabello *et al*, 2014). To date, approximately 40% of patients have no known pathogenic mutation. In this study, we carried out whole-exome sequencing (WES) analysis of 48 patients without known causative mutations or deletions and found loss-of function mutations in the *RPS27* and *RPL27* genes.

Methods

Patient samples

Genomic DNA (gDNA) was extracted from peripheral blood leucocytes with the QIAamp DNA Blood Mini Kit (QIAGEN, Hilden, Germany) according to the manufacturer's protocol. The diagnosis of DBA was based on the criteria developed at an international clinical consensus conference (Vlachos *et al*, 2008). All clinical samples were obtained with informed consent from paediatric and/or haematology departments throughout Japan. The Ethics Committee of Hirosaki University Graduate School of Medicine and the University of Tokyo approved this study.

Whole-exome sequencing analysis

To identify the candidate disease variants including non-RP genes, we performed WES analysis. gDNA from patients was enriched for protein-coding sequences with a SureSelect Human All Exon V3, V4 or V5 kit (Agilent Technologies, Santa Clara, CA, USA). This was followed by massively

parallel sequencing with the HiSeq 2000 platform with 100 bp paired-end reads (Illumina, San Diego, CA, USA). Candidate germline variants were detected through our in-house pipeline for WES analysis with minor modifications for the detection of germline variants (Yoshida *et al*, 2011; Kunishima *et al*, 2013). The resultant sequences were aligned to the University of California Santa Cruz (UCSC) Genome Browser hg19 with the Burrows-Wheeler Aligner (Li & Durbin, 2009). After removal of duplicate artifacts caused by polymerase chain reaction (PCR), the single nucleotide variants with an allele frequency >0·25 and insertion-deletions with an allele frequency >0·1 were called. With a mean depth of coverage of 116·3× (67× – 166×), more than 92% of the 50 Mb target sequences were analysed by more than 10 independent reads.

Target deep sequencing analysis was performed for the RP genes with a low depth of coverage of <10×. Amplification of the genome was accomplished by long PCR reactions using KOD-FX-Neo DNA polymerase (TOYOBO, Osaka, Japan) using the primers described in Data S1. The PCR products were used for library preparation after determination of their quantity by the Qubit dsDNA HS Assay (Life Technologies, Invitrogen division, Darmstadt, Germany). Libraries were prepared using the Nextera XT DNA Sample Preparation Kit (Illumina) according to the manufacturer's recommendation. Sequencing reactions were carried out using the MiSeq v2 (2 × 150 bp) chemistries (Illumina). The MiSeq re-sequencing protocol for amplicon was performed. The sequences were mapped on the human GRCh37/hg19 assembly and quality-checked using the on-board software MiSeq Reporter, and analysed by AVADIS NGS software (Agilent Technologies).

To validate *RPL27* and *RPS27* mutations of patients and their families, we performed direct sequencing analysis using the primers described in Data S1.

Cell lines and transient transfection with small interfering RNA

The human erythroleukaemic cell line K562 was maintained in RPMI 1640 medium (Sigma-Aldrich, St. Louis, MO, USA) supplemented with 10% fetal bovine serum (FBS) (Life Technologies, Carlsbad, CA, USA) at 37°C in a 5% CO_2 atmosphere. To knock down the *RPL27* and *RPS27* genes, cells were transfected by using Amaxa Nucleofector (Amaxa Biosystems, Gaithersburg, MD, USA) (Nucleofector solution V, Nucleofector program T-16) with 5 μl of 40 nmol/l siRNA solutions per 2 × 10^6 cells. The siRNA purchased from Thermo-Fisher Scientific-Dharmacon (Waltham, MA, USA) were ON-TARGET plus SMART pool human *RPS19, RPL5, RPS27, RPL27* and a non-targeting pool.

Northern blot analysis

Total RNA was extracted from cells using the RNeasy plus kit (QIAGEN), and hybridized at high stringency. The probes used in the present study are described in Data S1.

Functional analysis using zebrafish

Morpholino antisense oligonucleotides (MOs) targeting zebrafish *rpl27* and *rps27*, orthologs of human *RPL27* and *RPS27* respectively, were obtained from Gene Tools, LLC (Philomath, OR, USA). They were injected at a concentration of 5·0 or 20 μg/μl into one-cell-stage embryos. The MO-injected embryos (morphants) were grown at 28·5°C. Haemoglobin staining was performed at 48 h post-fertilization (hpf) using *o*-dianisidine (Uechi *et al*, 2006; Torihara *et al*, 2011).

Full-length *rpl27* was amplified by PCR and cloned into a pCS2+ vector for *in vitro* transcription. Capped mRNAs were synthesized from the linearized template using an mMessage mMachine SP6 kit (Life Technologies) and injected at 250 ng/μl into one-cell-stage embryos.

Total RNA was isolated from wild-types and the morphants. Reverse transcription (RT)-PCR was used to distinguish normal or cryptic sizes of the *rpl27* and *rps27.1* transcripts. This was performed by using primer pairs designed at exons 1 and 5 and exons 1 and 4, respectively. The MO and primer sequences are described in Data S1.

Results

Whole exome-sequencing analysis

A total of 98 Japanese DBA patients were registered and blood genomic DNA samples were collected. All samples were first screened for mutations in eight of 10 known DBA genes (*RPL5*, *RPL11*, *RPL35A*, *RPS10*, *RPS17*, *RPS19*, *RPS24* and *RPS26*) as well as *RPS14*, which had been implicated in the 5q- myelodysplastic syndrome, a subtype of myelodysplastic syndrome characterized by a defect in erythroid differentiation (Ebert *et al*, 2008). Screening was achieved by direct sequence analysis accompanied by high-resolution melt analysis (HRM) (Konno *et al*, 2010). Among these patients, 38% (38/100) had identifiable DBA mutations (Table S1). Some of the patients were described in our previous reports (Konno *et al*, 2010; Kuramitsu *et al*, 2012). Then, we screened for large gene deletions in the remaining 60 patients using synchronized-quantitative-PCR DBA gene copy number assay and/or genome wide single nucleotide polymorphism array analysis (Kuramitsu *et al*, 2012). We found that 20% (12 of 60) of samples had large deletions in previously identified DBA genes (Table S1).

WES was performed on the remaining 48 patients who lacked documented mutations or large deletions involving known DBA genes by screening. We found gene alterations in *RPS7*, *RPS27*, *RPL3L*, *RPL6*, *RPL7L1*, *RPL8*, *RPL13*, *RPL14*, *RPL18A*, *RPL27*, *RPL31* and *RPL35A* in 12 patients, whose WES data have been deposited in the European Genome-phenome Archive (EGA) under accession number EGAS00001000875. WES failed to identify a single *GATA1* mutation (Table I). The substitution mutations observed in

Table I. Characteristics of patients investigated by whole-exome sequencing.

Patient (*UPN*)	Age at diagnosis	Gender	Inheritance	Abnormalities	Mutation
5	1 year	F	Sporadic	None	*RPL18A* c.481C>T p.Arg161Cys
7	1 month	M	Sporadic	SGA, craniofacial abnormalities, skin pigmentation	ND
13	3 months	F	Sporadic	None	ND
21	1 year	F	Familial	None	*RPS7* c.75+1G>A Splicing error, *RPL13* c.547C>T p.R183C
26	Birth	F	Sporadic	Spastic quadriplegia, congenital hip dislocation, severe myopia, optic nerve hypoplasia, growth retardation	ND
35	18 months	M	Familial	None	*RPL6* c.253_255del p.Lys85del
36 (35 cousin)	Birth	M	Familial	Hypospadias, cryptorchidism	ND (No *RPL6* mutation was detected.)
37	4 years	M	Sporadic	Hypospadias, cryptorchidism, SGA	ND
42	2 months	F	Sporadic	None	*RPS27* c.89delC, p.Tyr31Thrfs*5
48	NA	NA	Sporadic	Fetal hydrops	*RPL3L* c.76C>G p.Arg26Gly
49	2 months	M	Sporadic	SGA, growth retardation	ND
50	2 months	F	Familial	Neutropenia	ND
52 (50 sister)	6 months	F	Familial	Neutropenia	ND
51	7 months	F	Sporadic	None	ND
53	8 months	F	Sporadic	SGA	ND
54	8 years	F	Sporadic	None	ND
61	9 months	M	Sporadic	None	ND
67	3 years	M	Sporadic	None	ND
68	16 months	M	Sporadic	None	*RPL14* c.446CTG(9), c.446CTG(15)
69	1 year	M	Sporadic	Flat thenar	ND
75	Birth	F	Familial	Acetabular dysplasia, total anomalous pulmonary venous connection	ND
76	Birth	M	Sporadic	IgG subclass 2 and 4 deficiency	*RPL35A* c.125A>G:p.Tyr42Cys *RPL7L1* c.G544A:p.V182I (His unaffected parents did not possess the mutation in *RPL35A*.)
77	Birth	M	Familial	None	ND
83	9 months	M	Sporadic	None	*RPL31* c.122G>A p.Arg41His
88	Birth	M	Familial	Cryptorchidism, hypospadias, learning disabilities	ND
89 (88 father)	NA	M	Familial	Skeletal malformation of fingers, growth retardation	ND
90	10 months	M	Sporadic	None	ND
91	Birth	F	Sporadic	None	*RPL8* c.413C>T p.Ser138Phe
93	11 months	M	Sporadic	Leucoderma, syndactyly	ND
95	Birth	F	Sporadic	Atrial septal defect, pulmonary stenosis	*RPL27* c.-2-1G>A Splicing error
96	28 months	F	Sporadic	None	ND
97	4 years	F	Sporadic	Growth retardation	ND
105	Birth	M	Sporadic	Growth retardation	ND
109	9 months	F	Sporadic	None	ND

Table I. (*Continued*)

Patient (UPN)	Age at diagnosis	Gender	Inheritance	Abnormalities	Mutation
112	4 months	F	Sporadic	Pulmonary atresia, tricuspid atresia, ventricular septal defect, hypoplasia of right ventricle, polydactyly of thumb, cerebellar hypoplasia, low-set ear, mandibular retraction, growth retardation	ND
116	4 months	M	Sporadic	Flat thenar	ND
117	NA	F	Sporadic	NA	ND
121	2 months	F	Sporadic	Growth retardation	ND
135	1 year	M	Sporadic	Xanthogranuloma	ND
136	Birth	M	Sporadic	None	ND
140	Birth	F	Sporadic	SGA	ND
144	2 months	F	Sporadic	Neutropenia	*RPL35A* c.125A>G p.Tyr42Cys (Her unaffected parents did not possess the mutation in *RPL35A*.)
151	9 months	M	Unknown	None	*RPL35A* c.113A>G p.Glu38Gly (His unaffected father was also heterozygous for the allele.)
152	NA	NA	Sporadic	None	ND
153	17 months	M	Sporadic	None	ND
154	NA	NA	NA	NA	ND
158	3 months	M	Sporadic	Patent ductus arteriosus	ND
159	8 months	M	Sporadic	None	ND

UPN, unique patient number; NA, not available; M, male; F, female; ND, not detected; SGA, small for gestational age.

RPL35A (Patients 76, 144 and 151) had escaped detection by the HRM analysis in the first step screening but were found by WES analysis. The mutations were confirmed by direct sequencing analysis. We speculated that the sensitivity of the HRM screening was insufficient for detection of these particular mutations because the size of the PCR amplicon containing the mutations was too large for the screening. A single missense mutation (c.125A>G: p.Tyr42Cys) observed in two of the sporadic DBA cases, Patients 76 and 144, was predicted to be causative because the unaffected parents of the two patients did not possess the mutation, suggesting that the mutations were *de novo* (Table I). Furthermore, tyrosine at position 42 is highly conserved among species. On the other hand, the pathological significance of the *RPL35A* mutation (c.113A>G p.Glu38Gly) observed in Patient 151 remains unknown because glutamic acid at position 38 is not well-conserved and the patient's unaffected father was also heterozygous for the allele (Table I).

The two known DBA genes, *RPS7* and *RPL26*, were not included in the first screening. Consequently, WES identified a *RPS7* mutation in Patient 21 and confirmed the mutation by direct sequencing. The mutation was predicted to be causative because it seemed to induce a splicing error in the gene. Mutations identified in the eight patients, including *RPL18A* in Patient 5, *RPL13* in Patient 21, *RPL6* in Patient 35, *RPL3L* in Patient 48, *RPL14* in Patient 68, *RPL7L1T* in Patient 76, *RPL31* in Patient 83 and *RPL8* in Patient 91, were missense mutations or in-frame deletions. Almost all of the causative variants of RP genes observed in DBA are loss-of function mutations (Gazda *et al*, 2012). Whereas analyses by SIFT, PolyPhen-2, Mutation Taster and CONDEL predicted that some of these mutations would probably damage the structure and function of ribosomal proteins, the pathological effects of the above-mentioned mutations were uncertain (Table S2). The substitution mutation of *RPL13* observed in Patient 21 seemed to be non-pathological because the *RPS7* splicing error mutation was also identified in this patient. The missense mutation in *RPL7L1T* found in Patient 76 also seemed to be non-pathological, because the *de novo* *RPL35A* mutation was identified in this patient. The in-frame deletion of *RPL6* observed in Patient 35 with familial DBA also might be non-causative, because the mutation was not identified in his cousin, Patient 36 (Table I).

De novo *mutation in* RPL27 *and* RPS27

Next, we focused on novel loss-of function mutations in *RPL27* and *RPS27*, found in the screening. Almost all RP genes were sequenced with enough coverage for detecting germline mutations except for several RP genes (Table S3). Target deep sequencing analysis was performed for the RP genes with a low depth of coverage of <10× (Table S4 and

S5), and we confirmed that the mutations in *RPL27* and *RPS27* were the only ones found in these patients.

In Patient 95, we identified the substitution of c.-2-1G>A in the *RPL27* gene, a putative splicing error mutation (Fig 1A). To confirm the effect of the mutation, we performed RT-PCR analysis by using primers located on the first and third exons and total RNA derived from the patient's leucocytes. We found two transcripts in Patient 95: the full-length transcript and a shorter transcript lacking exon 2 by alternative splicing, a variant skipping exon 2, in which the translation initiation codon is located (Fig 1B,C). We performed a quantitative assessment of the levels of the full-length transcripts and the short transcripts, using the Experion automated electrophoresis system (Bio-Rad, Hercules, CA, USA). The calculated concentration of each product was 48·31 nmol/μl (7·49 ng/μl) and 31·69 nmol/μl (3·19 ng/μl), respectively. The results indicated that the extent of aberrant splicing accounted for about 40% of total *RPL27* transcripts in this patient. Patient 95 was a 2-year-old girl with no family history of anaemia, diagnosed with DBA at birth. She had an atrial septal defect and pulmonary stenosis. She responded to corticosteroid treatment and has been in remission for 2 years. Her clinical characteristics are presented in Table II. As she was thought to be sporadic type DBA, we examined the genotype of her parents. The direct sequencing analysis showed that the parents were homozygous for wild-type *RPL27* (Fig 1A). These results suggested the mutation observed in the patient was *de novo* and a probable pathogenic mutation of DBA.

In Patient 42, we found a single nucleotide deletion (c.90delC, p.Tyr31Thrfs*5) in the *RPS27* gene generating a premature stop codon by frameshift (Fig 1D). The patient was a 4-year-old girl with no family history of anaemia, diagnosed with DBA at 2 months of age. This patient had no abnormalities except for skin pigmentation, and responded to steroid treatment. Her clinical characteristics are presented in Table II. Her unaffected parents did not have the gene alteration observed in the patients (Fig 1D), indicating the mutation was *de novo*.

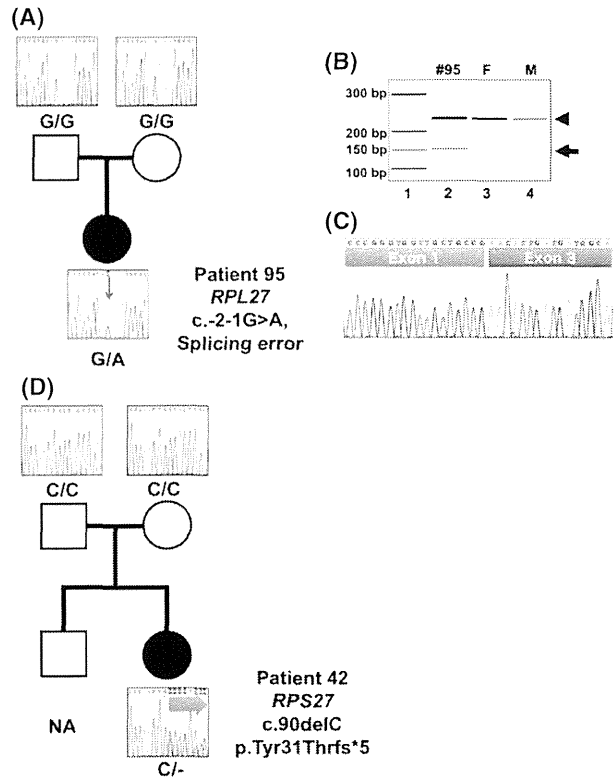

Fig 1. *De novo* mutations in *RPL27* and *RPS27*. (A) Family tree of Patient 95. Electropherograms indicate the gDNA sequence including the boundary between IVS-1 and the first exon of the *RPL27* gene. The red arrow indicates the position of the nucleotide substitution −2-1G>A observed in Patient 95. (B) RT-PCR analysis using the primer set located on the first and third exons of the *RPL27* gene. Arrowhead and arrow indicate PCR products for the full-length variant and the alternative splicing lacking the second exon, respectively. Molecular marker (lane 1), Patient 95 (lane 2), her father (F, lane 3) and mother (M, lane 4) are shown. (C) Sequence analysis of the short PCR product of Patient 95 showing the alternative splicing variants lacking the second exon. (D) Family tree of Patient 42. Electropherograms indicate gDNA sequence including a portion of the second exon of the *RPS27* gene. Blue arrow indicates the frameshift signals caused by single nucleotide deletion of c.90delC.

Defective pre-ribosomal RNA processing due to repression of RPL27 *or* RPS27

A single pre-ribosomal RNA (pre-rRNA), called 45S is processed into mature 28S, 18S and 5.8S rRNAs (Hadjiolova *et al*, 1993; Rouquette *et al*, 2005). Among the mature rRNAs, the 28S and 5.8S rRNAs associate with the large ribosomal subunit (60S) and the 18S rRNA associates with the small subunits (40S) of the ribosome. It has been reported that the mutations in RP genes observed in DBA cause defects in pre-rRNA processing. For example, the loss-of-function of the small subunit of RP affects maturation of 18S rRNA (Gazda *et al*, 2006, 2012; Choesmel *et al*, 2007; Flygare *et al*, 2007; Idol *et al*, 2007; Doherty *et al*, 2010). To validate the effects of the knockdown of *RPS27* or *RPL27* on erythroid lineage cells, we introduced siRNA into the human erythroid cell line K562 cells and analysed pre-rRNA processing by Northern blotting analysis.

Consistent with previous reports, decreased expression of *RPS19* was associated with a defect in rRNA processing characterized by a decrease in 18S-E rRNA with accumulation of a 21S rRNA precursor, and decreased expression of *RPS26* resulted in accumulation of a 26S rRNA precursor. Reduction of *RPS27* led to the accumulation of 30S rRNA and a decrease in the 21S rRNA and 18S-E rRNA (Fig 2). These findings suggest that RPS27 is also essential for 18S rRNA processing, although RPS27 involves rRNA processing associated with the small subunit at different stages from RPS19 and RPS26. In contrast, knockdown of *RPL27* caused accumulation of 32S rRNA, which is very similar to the effects by *RPL5* siRNA, suggesting that RPL27 is important for the

Table II. Clinical characteristics of DBA patients with *RPS27* or *RPL27* mutation.

UPN	42	95
Mutated gene	*RPS27*	*RPL27*
Age (years)	4	2
Gender	Female	Female
Family history of anaemia	No	No
Onset	2 months of age	At birth
Malformation	Skin pigmentation	Atrial septal defect pulmonary stenosis
Clinical data at onset		
RBC ($\times 10^{12}$/l)	1·38	2·17
Hb (g/l)	49	71
MCV (fl)	105	92·3
Reticulocytes (%)	0·17	0·1
WBC ($\times 10^{9}$/l)	11·68	5·5
Platelets ($\times 10^{9}$/l)	373	446
Bone marrow	Hyper cellularity, erythroid 1%	Normo-cellularity, erythroid 7·4%
Response to first steroid therapy	Yes	Yes
Present therapy	NA	NA

UPN, unique patient number; RBC, red blood cell count; WBC, white blood cell count; NA, not available.

maturation of 28S and 5.8S rRNAs (Fig 2). These findings showed that decreased expression of *RPS27* and *RPL27* perturbed pre-rRNA processing associated with the small and large subunits, respectively.

To accurately model the degree of ribosomal haploinsufficiency, we titrated the dose of the siRNA to obtain approximately 50% of the expression compared with wild-type cells (Figure S1A). For this experiment, we used 50% *RPS19*, *RPS26* and *RPL5* knocked-down cells as positive controls. However, the rRNA processing defects were not clearly observed under these conditions even in the positive controls (Figure S1B). These results suggested that a more accurate functional assay was necessary to investigate the pathological significance of these mutations. For that reason, we turned to the zebrafish model.

Impairment of erythroid development in rpl27 *and* rps27*-deficient zebrafish*

To investigate the effects of *RPL27* mutations in DBA, we knocked down the zebrafish ortholog (*rpl27*) using MOs and analysed the morphology and erythropoietic status during embryonic development. The coding region of *rpl27* shares 84% nucleotide and 96% amino acid identities with its human ortholog. Although gene duplication is common in zebrafish, available information from public databases suggests that *rpl27* exists as a single copy in the genome. We inhibited expression of this gene using an MO designed to target the 3′-splice site of the first intron that corresponded

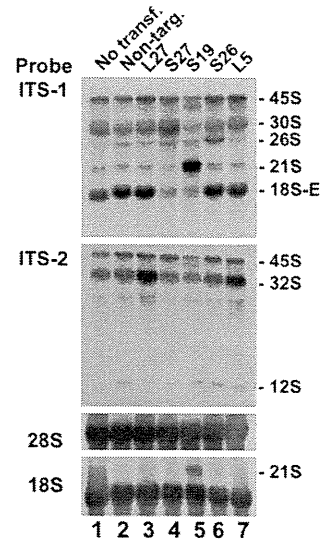

Fig 2. Perturbation of pre-rRNA processing by knockdown of the *RPL27* or *RPS27* gene. Northern blot analysis using K562 cells knocked down by siRNAs. The 5′ extremities of the internal transcribed spacer 1 (ITS-1) and internal transcribed spacer 2 (ITS-2) were used as probes to detect the precursors to the 18S rRNA associated with the small subunit and 28S rRNA and 5.8S rRNA associated with the large subunit of the ribosome, respectively. *RPS19*, *RPS26* and *RPL5* knocked-down cells were used as positive controls for the detection of defects in rRNA processing. ITS-1 and ITS-2 probes revealed the accumulation of 30S pre-rRNA in *RPS27* knocked-down cells and 32S pre-rRNA in *RPL27* knocked-down cells, respectively. Decrease of 18S-E pre-rRNA was also detected by the ITS-1 probe in *RPS27* knockdown cells. The mature 18S and 28S rRNAs were detected with specific probes.

to the position at which the mutation was identified in the patient (Fig 3A). Injection of this MO into the one-cell stage embryos perturbed the splicing and resulted in exclusion of exon 2 as observed in the patient (Fig 3B). When injected with 5 μg/μl MO targeted against *rpl27*, the expression level of a smaller transcript lacking exon 2 was comparable to that seen in Patient 1 (Figs 1B and 3B). Therefore, all of the following experiments were performed using 5 μg/μl MO.

We compared the morphological features of the morphants with wild-type embryos and found that the morphants showed abnormal phenotypes, such as a thin yolk sac extension and a bent tail at 25 hpf (Fig 3C). We also performed haemoglobin staining at 48 hpf and found a marked reduction of erythrocyte production in the cardial vein of the morphants (Fig 3D). All these abnormalities were rescued by the simultaneous injection of *rpl27* mRNA into the embryos, indicating that the morphological defects and decreased erythropoiesis observed in the morphants were caused by the aberrant splicing of *rpl27* in zebrafish (Fig 3B,D). These results suggested that the splice site mutation identified in human *RPL27* could be responsible for the pathogenesis of DBA.

We next investigated the effects of *RPS27* mutations in DBA. Public databases suggest that there are three copies of the zebrafish *rps27* gene, *rps27.1*, *rps27.2* and *rps27.3*, whereas

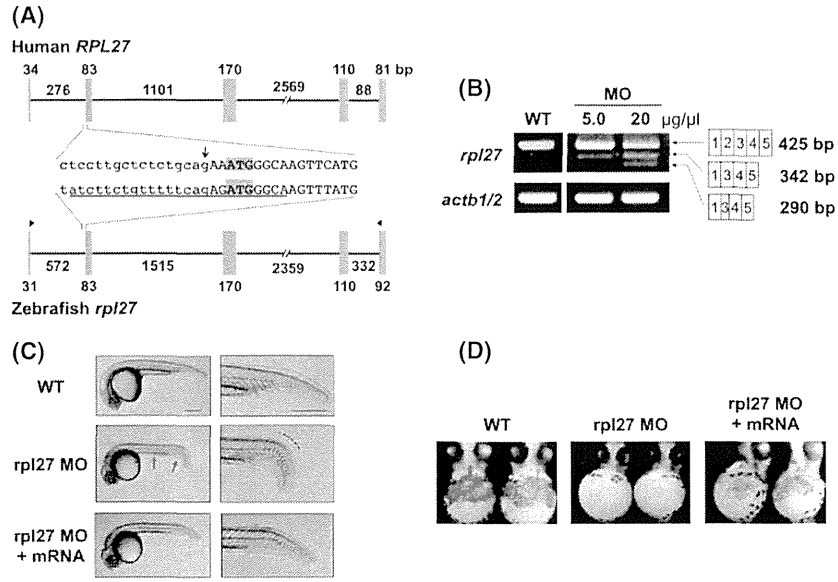

Fig 3. Morphological defects and decreased erythropoiesis in *rpl27* morphants. (A) The gene structures of human *RPL27* and zebrafish *rpl27*. The sequences of intron 1/exon 2 boundary regions are indicated. Uppercase and lowercase letters show the exon and intron sequences, respectively. The MO target site is underlined and the translation initiation codons (ATG) are shaded. The arrow indicates the position of the mutated nucleotide in the patient. Arrowheads show the primer positions for the RT-PCR. (B) The results of RT-PCR of *rpl27* and *actb* (control) in wild type and MO injected embryos. A smaller transcript without exon 2 was observed in the morphants as seen in the patient at a comparable level, when 5 μg/μl MO was injected into the one-cell-stage embryos. Injection with higher concentrations of MO (20 μg/μl) also produced a truncated exon 3. (C) Morphological features of wild-type and MO-injected embryos. A thin yolk sac extension and a bent tail are prominent in the morphants injected with 5 μg/μl MO (arrows), whereas these features are rescued in the embryos injected with *rpl27* mRNA. Scale bars: 250 μm. (D) The haemoglobin staining of cardial veins at 48 hpf. Compared to wild-type embryos, *rpl27* morphants injected with 5 μg/μl MO showed a drastic reduction in the number of haemoglobin-stained blood cells. Morphants co-injected with *rpl27* mRNA show recovery of the stained cells.

the human genome contains two copies, *RPS27* and *RPS27L*. We inhibited expression of the zebrafish *rps27.1*, which shares 96% amino acid identity with the human *RPS27*, using an MO designed to target the 5′-splice site of the second intron (Fig 4A). Injection of this MO into the embryos perturbed the splicing and resulted in exclusion of exon 2 (Fig 4B) that consequently introduced a stop codon in exon 3. The morphants showed abnormal phenotypes, such as a thin yolk sac extension, a bent tail and a malformed brain region at 26 hpf (Fig 4C). We also observed reduced erythrocyte production in about 60% of the morphants (Fig 4D). These results suggested that the frameshift mutation identified in human *RPS27* is a strong candidate for a causative mutation for DBA.

Discussion

WES analysis identified loss-of-function mutations in two RP genes. Each of the patients carrying one of these mutations was a sporadic case, and the mutations were *de novo*. Knockdown of *RPL27* and *RPS27* disturbed pre-rRNA processing for the large and small subunits, respectively. Although the zebrafish models cannot reproduce the exact features of DBA, such as macrocytic anaemia appearing after birth and skeletal abnormalities, the models of *RPL27* and *RPS27* mutations showed impairment of erythrocyte production. These results suggested that *RPL27* and *RPS27* play important roles in erythropoiesis, and that haploinsufficiency of either RP could lead to pure red cell aplasia. However, these findings only represent a single patient in relation to each gene. The identification of new DBA cases in the future with mutations in these genes will be important to confidently label *RPS27* and *RPL27* as DBA disease genes.

Interestingly, RPS27 binds to MDM2 through its N-terminal region, and overexpression of RPS27 stabilizes TP53 by inhibiting MDM2-induced TP53 ubiquitination (Xiong *et al*, 2011). Although the exact mechanism by which ribosome disruptions leads to DBA is unclear, a widely accepted hypothesis is that imbalances in expression of individual RPs trigger a TP53-mediated checkpoint, leading to cell cycle arrest and apoptosis of erythroid precursors (Narla & Ebert, 2010). Several animal models have demonstrated the role of TP53 in the pathophysiology of DBA (McGowan & Mason, 2011). In support of this conclusion, it was observed that certain RPs, such as RPL5, RPL11, RPL23, RPL26 and RPS7, bind to and inhibit the TP53 regulator MDM2, thereby inhibiting its ability to promote TP53 degradation (Zhang & Lu, 2009). Notably, like *RPL27*, many of the RP genes, including *RPL5*, *RPL11*, *RPL26* and *RPS7*, are mutated in DBA.

Here, we report the results of RP gene mutations observed in 98 Japanese DBA patients. The frequency of the patients harbouring probable causative mutations/large

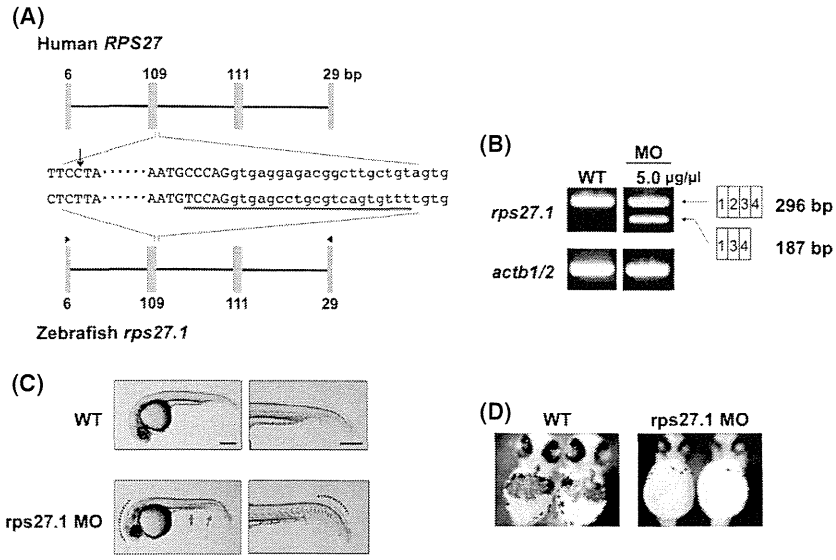

Fig 4. Morphological defects and decreased erythropoiesis in *rps27* morphants. (A) The gene structures of human *RPS27* and zebrafish *rps27.1*. The sequences of exon 2/intron 2 boundary regions are indicated. Uppercase and lowercase letters show the exon and intron sequences, respectively. The MO target site is underlined. The arrow indicates the position of the mutated nucleotide in the patient. Arrowheads show the primer positions for RT-PCR. (B) The results of RT-PCR of *rps27.1* and *actb* (control) in wild-type and MO-injected embryos. A smaller transcript without exon 2 was observed in the morphants. (C) Morphological features of wild-type and MO-injected embryos at 26 hpf. A thin yolk sac extension and a bent tail are prominent in the morphants (arrows). An abnormal development in the brain region was also observed. Scale bars: 250 μm. (D) Haemoglobin staining of cardial veins at 48 hpf.

deletions in RP genes was 55% (56/98), including *RPS19* 16% (16), *RPL5* 12% (12), *RPL11* 5% (5), *RPS17* 7% (7), *RPL35A* 7% (7), *RPS26* 4% (4), *RPS10* 1% (1), *RPS7* 1% (1), *RPL27* 1% (1) and *RPS27* 1% (1). No mutation of *RPS24*, *RPS29* or *RPL26* was identified in this study. In addition to above mutations, we found a missense mutation of *RPL35A* in a sporadic case (Patient 151). Mutations in RP genes are characterized by a wide variability of phenotypic expression. Even family members with the same mutation in the RP gene can present with clinical differences (Willig *et al*, 1999). For example, *RPS19* mutations are found in some first-degree relatives presenting only with isolated high erythrocyte adenosine deaminase activity and/or macrocytosis. Therefore, there is still the possibility that this *RPL35A* mutation is disease-causing, although the patients' father had the same heterozygous mutation without anaemia. To confirm the pathological effect of the substitution, a functional analysis is necessary. The zebrafish model might be very useful for this assay.

Recently, Gerrard *et al* (2013) found inactivating mutations in 15/17 patients by targeted sequencing of 80 RP genes. All mutations were in genes previously found to be DBA genes. The differences between these results and those in our study might be due to differences between human populations. In our cohort, all patients were Asian, whereas 80% were Caucasian in the cohort reported by Gerrard *et al* (2013). The frequency of RP gene mutaitons may vary between ethnic groups. However, the data from both cohorts are based on a relatively low number of patients and values showing significant differences between cohorts are missing. Interestingly, Gazda *et al* (2012) reported large-scale sequencing of 79 RP genes in a cohort of 96 DBA probands, none of whom had previously been found to have a pathogenic mutation. The study showed *c.* 53·9% of DBA patients had mutations in one of 10 known DBA-associated RP genes, including a novel causative *RPL26* gene. The results were very similar to ours, although their data did not contain large deletions of RP genes, which would escape regular sequencing analysis.

An additional five missense single nucleotide variants affecting single cases were identified in six patients, including *RPL3L*, *RPL7L1*, *RPL8*, *RPL13*, *RPL18A* and *RPL31* together with two in-frame deletions of *RPL6* and *RPL14* in two patients, which cause deletion of a single amino-acid (Table I). However, the pathological significance in these seven cases is uncertain. In the remaining 36 patients, no mutations were detected in *RP* genes. In conclusion, we identified novel germline mutations of two RP genes that could be responsible for DBA, further confirming the concept that RP genes are common targets of germline mutations in DBA patients and also suggesting the presence of non-RP gene targets for DBA. To identify the candidate disease variants in non-RP genes, we are now pursuing WES of their parents and planning to perform functional assays of these variants.

Acknowledgements

We thank T. Kudo and A. Mikami for their technical assistance. This work was supported by the Research on Measures for Intractable Diseases Project and Health and Labor

Sciences Research grants (Research on Intractable Diseases) from the Ministry of Health, Labour and Welfare, by Grants-in-Aid from the Ministry of Health, Labour and Welfare of Japan and by grants-in-aid for scientific research from the Ministry of Education, Culture, Sports, Science and Technology of Japan (KAKENHI: 25291003).

Authorship and Disclosure

Y.O., Y. S., A.S.-O., K.C., H.T. and S.M. performed bioinformatics analyses of the resequencing data. R.W., K.Y., T.T. and R.K. processed and analysed genetic material, prepared the library and performed sequencing. R.W., K.Y., T.T. and R.K. performed the Northern blot analyses and RT-PCR analyses. M.K and I.H. performed DBA copy number analysis. T. S., T. U. and N.K. performed zebrafish experiments. K. K., I.K., S. Ohga, A.O., J.H., K.S., K.M., K. K., A.I., Y. K., S.K., K.T., T. S. and E.I. collected specimens and were involved in planning the project. Y.I. and H.K. analysed data and designed the study. E.I. and S.O led the entire project. T.T., R.W., N.K. and I.E. wrote the manuscript. All authors participated in discussions and interpretation of the data and results.

Supporting Information

Additional Supporting Information may be found in the online version of this article:

Fig S1. Perturbation of pre-rRNA processing by knockdown of the *RPL27* or *RPS27* gene when the extent of the knockdown was approximately 50%.

Data S1. Methods.

Table S1. Mutations identified in *RPS19*, *RPL5*, *RPL11*, *RPL35A*, *RPS17* and *RPS26* in Japanese DBA patients.

Table S2. Prediction of functional effects of mutations in ribosomal protein genes.

Table S3. Mean coverage of whole-exome sequencing of RP genes in Patients #42 and #95.

Table S4. Average coverage of target deep sequencing of RP genes in Patient #95.

Table S5. Average coverage of target deep sequencing of RP genes in Patient #42.

References

Choesmel, V., Bacqueville, D., Rouquette, J., Noaillac-Depeyre, J., Fribourg, S., Crétien, A., Leblanc, T., Tchernia, G., Da Costa, L. & Gleizes, P.E. (2007) Impaired ribosome biogenesis in Diamond-Blackfan anemia. *Blood*, **109**, 1275–1283.

Cmejla, R., Cmejlova, J., Handrkova, H., Petrak, J. & Pospisilova, D. (2007) Ribosomal protein S17 gene (RPS17) is mutated in Diamond-Blackfan anemia. *Human Mutation*, **28**, 1178–1182.

Doherty, L., Sheen, M.R., Vlachos, A., Choesmel, V., O'Donohue, M.F., Clinton, C., Schneider, H.E., Sieff, C.A., Newburger, P.E., Ball, S.E., Niewiadomska, E., Matysiakm M, Glader., B., Arceci., R.J., Farrar., J.E., Atsidaftosm.E., Liptonm J, M., Gleizes, P.E. & Gazda, H.T. (2010) Ribosomal protein genes RPS10 and RPS26 are commonly mutated in Diamond-Blackfan anemia. *The American Journal of Human Genetics*, **86**, 222–228.

Draptchinskaia, N., Gustavsson, P., Andersson, B., Pettersson, M., Willig, T.N., Dianzani, I., Ball, S., Tchernia, G., Klar, J., Matsson, H., Tentler, D., Mohandas, N., Carlsson, B. & Dahl, N. (1999) The gene encoding ribosomal protein S19 is mutated in Diamond-Blackfan anaemia. *Nature Genetics*, **21**, 169–175.

Ebert, B.L., Pretz, J., Bosco, J., Chang, C.Y., Tamayo, P., Galili, N., Raza, A., Root, D.E., Attar, E., Ellis, S.R. & Golub, T.R. (2008) Identification of RPS14 as a 5q- syndrome gene by RNA interference screen. *Nature*, **451**, 335–339.

Farrar, J.E., Nater, M., Caywood, E., McDevitt, M.A., Kowalski, J., Takemoto, C.M., Talbot, C.C. Jr, Meltzer, P., Esposito, D., Beggs, A.H., Schneider, H.E., Grabowska, A., Ball, S.E., Niewiadomska, E., Sieff, C.A., Vlachos, A., Atsidaftos, E., Ellis, S.R., Lipton, J.M., Gazda, H.T. & Arceci, R.J. (2008) Abnormalities of the large ribosomal subunit protein, Rpl35a, in Diamond-Blackfan anemia. *Blood*, **112**, 1582–1592.

Flygare, J., Aspesi, A., Bailey, J.C., Miyake, K., Caffrey, J.M., Karlsson, S. & Ellis, S.R. (2007) Human RPS19, the gene mutated in Diamond-Blackfan anemia, encodes a ribosomal protein required for the maturation of 40S ribosomal subunits. *Blood*, **109**, 980–986.

Gazda, H.T., Grabowska, A., Merida-Long, L.B., Latawiec, E., Schneider, H.E., Lipton, J.M., Vlachos, A., Atsidaftos, E., Ball, S.E., Orfali, K.A., Niewiadomska, E., Da Costa, L., Tchernia, G., Niemeyer, C., Meerpohl, J.J., Stahl, J., Schratt, G., Glader, B., Backer, K., Wong, C., Nathan, D.G., Beggs, A.H. & Sieff, C.A. (2006) Ribosomal protein S24 gene is mutated in Diamond-Blackfan anemia. *The American Journal of Human Genetics*, **2006**, 1110–1118.

Gazda, H.T., Sheen, M.R., Vlachos, A., Choesmel, V., O'Donohue, M.F., Schneider, H., Darras, N., Hasman, C., Sieff, C.A., Newburger, P.E., Ball, S.E., Niewiadomska, E., Matysiak, M., Zaucha, J.M., Glader, B., Niemeyer, C., Meerpohl, J.J., Atsidaftos, E., Lipton, J.M., Gleizes, P.E. & Beggs, A.H. (2008) Ribosomal protein L5 and L11 mutations are associated with cleft palate and abnormal thumbs in Diamond-Blackfan anemia patients. *The American Journal of Human Genetics*, **83**, 769–780.

Gazda, H.T., Preti, M., Sheen, M.R., O'Donohue, M.F., Vlachos, A., Davies, S.M., Kattamis, A., Doherty, L., Landowski, M., Buros, C., Ghazvinian, R., Sieff, C.A., Newburger, P.E., Niewiadomska, E., Matysiak, M., Glader, B., Atsidaftos, E., Lipton, J.M., Gleizes, P.E. & Beggs, A.H. (2012) Frameshift mutation in p53 regulator RPL26 is associated with multiple physical abnormalities and a specific pre-ribosomal RNA processing defect in diamond-blackfan anemia. *Human Mutation*, **33**, 1037–1044.

Gerrard, G., Valgañón, M., Foong, H.E., Kasperaviciute, D., Iskander, D., Game, L., Müller, M., Aitman, T.J., Roberts, I., de la Fuente, J., Foroni, L. & Karadimitris, A. (2013) Target enrichment and high-throughput sequencing of 80 ribosomal protein genes to identify mutations associated with Diamond-Blackfan anaemia. *British Journal of Haematology*, **162**, 530–536.

Hadjiolova, K.V., Nicoloso, M., Mazan, S., Hadjiolov, A.A. & Bachellerie, J.P. (1993) Alternative pre-rRNA processing pathways in human cells and their alteration by cycloheximide inhibition of protein synthesis. *European Journal of Biochemistry*, **212**, 211–215.

Idol, R.A., Robledo, S., Du, H.Y., Crimmins, D.L., Wilson, D.B. & Ladenson, J.H. (2007) Cells depleted for RPS19, a protein associated with Diamond Blackfan anemia, show defects in 18S ribosomal RNA synthesis and small ribosomal subunit production. *Blood Cells Molecules and Diseases*, **39**, 35–43.

Ito, E., Konno, Y., Toki, T. & Terui, K. (2010) Molecular pathogenesis in Diamond-Blackfan anemia. *International Journal of Hematology*, **92**, 413–418.

Konno, Y., Toki, T., Tandai, S., Xu, G., Wang, R.N., Terui, K., Ohga, S., Hara, T., Hama, A., Kojima, S., Hasegawa, D., Kosaka, Y., Yanagisawa, R., Koike, K., Kanai, R., Imai, T., Hongo, T., Park, M.J., Sugita, K. & Ito, E. (2010) Mutations in the ribosomal protein genes in Japanese patients with Diamond-Blackfan anemia. *Haematologica*, **95**, 1293–1299.

Kunishima, S., Okuno, Y., Yoshida, K., Shiraishi, Y., Sandada, M., Muramatsu, H., Chiba, K., Tanaka, H., Miyazaki, K., Sakai, M., Ohtake, M., Kobayashi, R., Iguchi, A., Niimi, G., Otsu, M., Takahashi, Y., Miyano, S., Saito, H., Kojima, S. & Ogawa, S. (2013) ACTN1 mutations cause congenital macrothrombocytopenia. *The American Journal of Human Genetics*, **92**, 431–438.

Kuramitsu, M., Sato-Otsubo, A., Morio, T., Takagi, M., Toki, T., Terui, K., Wang, R., Kanno, H., Ohga, S., Ohara, A., Kojima, S., Kitoh, T., Goi, K., Kudo, K., Matsubayashi, T., Mizue, N., Ozeki, M., Masumi, A., Momose, H., Takizawa, K., Mizukami, T., Yamaguchi, K., Ogawa, S., Ito, E. & Hamaguchi, I. (2012) Extensive gene deletions in Japanese patients with Diamond-Blackfan anemia. *Blood*, **119**, 2376–2384.

Li, H. & Durbin, R. (2009) Fast and accurate short read alignment with Burrows-Wheeler transform. *Bioinformatics*, **25**, 1754–1760.

Lipton, J.M., Atsidaftos, E., Zyskind, I. & Vlachos, A. (2006) Improving clinical care and elucidating the pathophysiology of Diamond Blackfan anemia: an update from the Diamond Blackfan Anemia Registry. *Pediatric Blood & Cancer*, **46**, 558–564.

McGowan, K.A. & Mason, P.J. (2011) Animal models of Diamond Blackfan anemia. *Seminars in Hematology*, **48**, 106–116.

Mirabello, L., Macari, E.R., Jessop, L., Ellis, S.R., Myers, T., Giri, N., Taylor, A.M., McGrath, K.E., Humphries, J.M., Ballew, B.J., Yeager, M., Boland, J.F., He, J., Hicks, B.D., Burdett, L., Alter, B.P., Zon, L. & Savage, S.A. (2014) Whole-exome sequencing and functional studies identify RPS29 as a novel gene mutated in multi-case Diamond-Blackfan anemia families. *Blood*, **124**, 24–32.

Narla, A. & Ebert, B.J. (2010) Ribosomepathies: human disorders of ribosome dysfunction. *Blood*, **115**, 3196–3205.

Rouquette, J., Choesmel, V. & Gleizes, P.E. (2005) Nuclear export and cytoplasmic processing of precursors to the 40S ribosomal subunits in mammalian cells. *EMBO Journal*, **24**, 2862–2872.

Sankaran, V.G., Ghazvinian, R., Do, R., Thiru, P., Vergilio, J.A., Beggs, A.H., Sieff, C.A., Orkin, S.H., Nathan, D.G., Lander, E.S. & Gazda, H.T. (2012) Exome sequencing identifies *GATA1* mutations resulting Diamond-Blackfan anemia. *The Journal of Clinical Investigation*, **122**, 2439–2443.

Torihara, H., Uechi, T., Chakraborty, A., Shinya, M., Sakai, N. & Kenmochi, N. (2011) Erythropoiesis failure due to RPS19 deficiency is independent of an activated Tp53 response in a zebrafish model of Diamond-Blackfan anaemia. *British Journal of Haematology*, **152**, 648–654.

Uechi, T., Nakajima, Y., Nakao, A., Torihara, H., Chakraborty, A., Inoue, K. & Kenmochi, N. (2006) Ribosomal protein gene knockdown causes developmental defects in zebrafish. *PLoS ONE*, **1**, e37.

Vlachos, A., Ball, S., Dahl, N., Alter, B.P., Sheth, S., Ramenghi, U., Meerpohl, J., Karlsson, S., Liu, J.M., Leblanc, T., Paley, C., Kang, E.M., Leder, E.J., Atsidaftos, E., Shimamura, A., Bessler, M., Glader, B. & Lipton, J.M. (2008) Diagnosing and treating Diamond Blackfan anaemia: results of an international clinical consensus conference. *British Journal of Haematology*, **142**, 859–876.

Vlachos, A., Rosenberg, P.S., Atsidaftos, E., Alter, B.P. & Lipton, J.M. (2012) Incidence of neoplasia in Diamond Blackfan anemia: a report from the Diamond Blackfan Anemia Registry. *Blood*, **119**, 3815–3819.

Willig, T.N., Draptchinskaia, N., Dianzani, I., Ball, S., Niemeyer, C., Ramenghi, U., Orfali, K., Gustavsson, P., Garelli, E., Brusco, A., Tiemann, C., Pérignon, J.L., Bouchier, C., Cicchiello, L., Dahl, N., Mohandas, N. & Tchernia, G. (1999) Mutations in ribosomal protein S19 gene and diamond blackfan anemia: wide variations in phenotypic expression. *Blood*, **94**, 4294–4306.

Xiong, X., Zhao, Y., He, H. & Sun, Y. (2011) Ribosomal protein S27-like and S27 interplay with p53-MDM2 axis as a target, a substrate and a regulator. *Oncogene*, **30**, 1798–1811.

Yoshida, K., Sanada, M., Shiraishi, Y., Nowak, D., Nagata, Y., Yamamoto, R., Sato, Y., Sato-Otsubo, A., Kon, A., Nagasaki, M., Chalkidis, G., Suzuki, Y., Shiosaka, M., Kawahata, R., Yamaguchi, T., Otsu, M., Obara, N., Sakata-Yanagimoto, M., Ishiyama, K., Mori, H., Nolte, F., Hofmann, W.K., Miyawaki, S., Sugano, S., Haferlach, C., Koeffler, H.P., Shih, L.Y., Haferlach, T., Chiba, S., Nakauchi, H., Miyano, S. & Ogawa, S. (2011) Frequent pathway mutations of splicing machinery in myelodysplasia. *Nature*, **478**, 64–69.

Zhang, Y. & Lu, H. (2009) Signaling to p53: ribosomal proteins find their way. *Cancer Cell*, **16**, 369–377.

Simple and Efficient Generation of Virus-specific T Cells for Adoptive Therapy Using Anti-4-1BB Antibody

Nobuhiko Imahashi,† Tetsuya Nishida,* Tatsunori Goto,* Seitaro Terakura,* Keisuke Watanabe,* Ryo Hanajiri,* Reona Sakemura,* Misa Imai,* Hitoshi Kiyoi,* Tomoki Naoe,* and Makoto Murata**

Summary: Although recent studies of virus-specific T-cell (VST) therapy for viral infections after allogeneic hematopoietic stem cell transplantation have shown promising results, simple and less time-intensive and labor-intensive methods are required to generate VSTs for the wider application of VST therapy. We investigated the efficacy of anti-CD28 and anti-4-1BB antibodies, which can provide T cells with costimulatory signals similar in strength to those of antigen-presenting cells, in generating VSTs. When peripheral blood mononuclear cells were stimulated with viral peptides together with isotype control, anti-CD28, or anti-4-1BB antibodies, anti-4-1BB antibodies yielded the highest numbers of VSTs, which were on an average 7.9 times higher than those generated with isotype control antibody. The combination of anti-CD28 and anti-4-1BB antibodies did not result in increased numbers of VSTs compared with anti-4-1BB antibody alone. Importantly, the positive effect of anti-4-1BB antibody was observed regardless of the epitopes of the VSTs. In contrast, the capacity of dendritic cells (DCs) to generate VSTs differed considerably depending on the epitopes of the VSTs. Furthermore, the numbers of VSTs generated with DCs were at most similar to those generated with the anti-4-1BB antibody. Generation of VSTs with anti-4-1BB antibody did not result in excessive differentiation or deteriorated function of the generated VSTs compared with those generated with control antibody or DCs. In conclusion, VSTs can be generated rapidly and efficiently by simply stimulating peripheral blood mononuclear cells with viral peptide and anti-4-1BB antibody without using antigen-presenting cells. We propose using anti-4-1BB antibody as a novel strategy to generate VSTs for adoptive therapy.

Key Words: virus-specific T-cell therapy, anti-4-1BB antibody, costimulatory signals, antigen-presenting cells

(*J Immunother* 2015;38:62–70)

Allogeneic hematopoietic stem cell transplantation (HSCT) is a potentially curative therapy for patients with various hematologic diseases who are otherwise incurable with conventional therapies, albeit at the expense of high treatment–related mortality. Viral infections such as cytomegalovirus (CMV), Epstein-Barr virus (EBV), and adenovirus (AdV) infections are one of the major contributors to this high mortality.[1] Although antiviral agents are effective against some of the viruses, their efficacy is often limited by weak intrinsic activity against viruses and by their toxicity.[1] Furthermore, reconstitution of virus-specific T cells (VSTs) is important for the control of viral infections.[2] These observations have led to the development of adoptive T-cell therapy for the management of viral infections after allogeneic HSCT. Although the results of recent clinical studies that evaluated the safety and efficacy of VST therapy for viral infections after HSCT are promising,[3,4] several issues remain to be resolved. One of these issues is that generation of VSTs is complex and requires a large amount of time and effort.

Optimal activation of T cells requires not only engagement of the T-cell receptor (TCR) complex, but also a secondary signal that is provided by costimulatory molecules. A number of studies that analyzed the effect of costimulatory signals on T cells using artificial antigen-presenting cells (APCs) expressing costimulatory molecules have shown that costimulatory signals, especially signals through CD28 and 4-1BB, enhance the expansion of VSTs ex vivo.[5–7] Therefore, APCs that express costimulatory molecules are used to generate VSTs for adoptive therapy. Dendritic cells (DCs) are traditional APCs and are widely used to generate antigen-specific T cells for adoptive immunotherapy.[8,9] However, the preparation of DCs requires additional time (approximately 1 wk), effort, and peripheral blood mononuclear cells (PBMCs). Another type of APC that is commonly used is an artificial APC, which is genetically modified to express costimulatory molecules and human leukocyte antigen (HLA) molecules.[10] Although artificial APCs are easy to prepare, once they are generated they can only generate antigen-specific T cells that recognize peptides presented on the same HLA as that expressed on the artificial APC. Thus, artificial APCs cannot be universally used. In addition, virus vectors are required to generate artificial APCs. These issues associated with APCs account for, at least in part, the complexity and the time-intensive and labor-intensive nature of VST therapy. As B cells and monocytes contained in PBMCs have the capacity to present antigen to T cells, one possible solution to the previous limitations to VST generation may be to directly stimulate PBMCs with viral peptides.[11] However, as freshly isolated B cells and monocytes only express low levels of costimulatory molecules,[12,13] the costimulatory signals delivered to T cells when using this method may not be sufficient. Therefore, a simple and less time-intensive and labor-intensive method that provides T cells with sufficient costimulatory signals needs to be developed for the wider application of VST therapy.

Recent advances in the understanding of T-cell biology and in technology have led to the development of immunostimulatory antibodies such as anti-CD28 and

Received for publication October 21, 2014; accepted November 14, 2014.

From the *Department of Hematology and Oncology, Nagoya University Graduate School of Medicine, Nagoya; and †Japan Society for the Promotion of Science (JSPS), Japan.

Reprints: Tetsuya Nishida, Department of Hematology and Oncology, Nagoya University Graduate School of Medicine, 65 Tsurumai-cho, Showa-ku, Nagoya, Aichi 466-8550, Japan (e-mail: tnishida@med.nagoya-u.ac.jp).